Research Square

Preprints are preliminary reports that have not undergone peer review.
They should not be considered conclusive, used to inform clinical practice,
or referenced by the media as validated information.

Modeling and Optimization of Mobile Charging Operations in Electric Free-Floating Carsharing Systems

Lukas Verboven
Tai-Yu Ma
tai-yu.ma@liser.lu

Luxembourg Institute of Socio-Economic Research
Malvika Dixit
Luxembourg Institute of Socio-Economic Research

Research Article

Keywords: carsharing, electric vehicle, mobile charging system, rebalancing, node-charge graph

Posted Date: November 19th, 2026

DOI: https://doi.org/10.21203/rs.3.rs-11092473/v1

License: This work is licensed under a Creative Commons Attribution 4.0 International License.
Read Full License

Additional Declarations: No competing interests reported.

Modeling and Optimization of Mobile Charging Operations in Electric Free-Floating Carsharing Systems

Abstract

Mobile charging trucks (MCTs) offer a flexible complement to fixed charging stations by providing charging capacity where and when it is needed. However, their integration into electric free-floating carsharing (FFCS) operations require charging decisions to be coordinated with vehicle relocation and future vehicle availability.. This study develops a new mixed-integer linear programming model based on a node-charge graph that jointly optimizes the relocation and charging of idle vehicles, the positioning of MCTs, and the allocation of charging operations between fixed stations and MCTs. The objective minimizes a weighted combination of customer access time, EV relocation and charging time, MCT relocation time, and EV waiting time for charging. We assess the system performance with and without MCTs under various scenarios. The computational results on a Manhattan-like 60-zone area using synthetic data indicate that integrating one and two MCTs reduces the objective value by 10.74% and 14.09%, respectively, primarily through lower customer access times. The results also indicate that the relative benefit of MCTs diminishes as the idle EV fleet grows and increases when EV supply is spatially misaligned with customer demand. These findings demonstrate the potential operational value of coordinating mobile and fixed charging resources in electric FFCS systems while highlighting the need for empirical validation and further development for large-scale, real-time applications.

Keywords*: carsharing, electric vehicle, mobile charging* system*, rebalancing, node-charge graph*

1. Introduction

Carsharing is an important component of urban mobility and can reduce both car ownership and car use. In the Netherlands, car ownership among car sharers was more than 30% lower compared to before they joined carsharing (Nijland and Van Meerkerk, 2017). Well-known examples of carsharing operators, including Cambio, Share Now, and Zipcar, provide users with access to a large fleet of shared vehicles located at designated stations throughout the city. Users can reserve vehicles through a mobile application, pick them up, and return them at designated stations (station-based) or at any legal parking space within an operating area (free-floating carsharing (FFCS)). To further extend the environmental benefits of carsharing, many operators have introduced electric vehicles (EVs). Compared with internal combustion engine vehicles (ICEVs), EV-based fleets can produce significantly lower CO_2 emissions while satisfying the same demand, but require more charging infrastructure and have a significantly limited driving range (Fassio et al., 2021). Their charging operations must therefore be carefully managed.

For EV charging infrastructure, fixed charging stations remain the most widely adopted solution. Existing studies mainly focus on fixed charging station-based systems by considering the trade-off between EV downtime for charging and relocation (Roni et al., 2019; Pantelidis et al., 2022). An emerging flexible charging solution is considering mobile charging trucks/vehicles (MCTs) as a complementary mobile charging resource to enhance the efficiency of the fixed-charging-stations-based system. MCTs can travel to the locations of EVs instead of requiring the vehicles to travel to a fixed charging station. These trucks are equipped with a battery energy storage system and can provide charging at different locations within the operating area (Afshar et al., 2020). By bringing the charging service to the EVs, MCTs can reduce the need for relocation trips to fixed charging stations and potentially decrease the EV downtime for charging operations. By combining fixed charging stations with MCTs, the charging operations become more flexible, as MCTs can complement the fixed charging stations by providing additional charging capacity where and when it is needed. In this way, MCTs can help reduce waiting times and potential inefficiencies associated with fixed charging stations.

In EV-based FFCS systems, charging decisions are not only energy-management decisions; they also affect where vehicles are available for future users. Sending an EV to a fixed charging station may restore its battery but can remove it from a high-demand area. MCTs can reduce this trade-off, but only if their movements are coordinated with EV relocation and charging decisions. However, **it is still unclear how and**

when they should be integrated into FFCS systems and under what conditions this increases operational flexibility compared to fixed charging stations. Existing literature studies EV relocation with EV charging mainly based on fixed charging stations, but integrating MCTs into FFCS charging management remains underexplored. This paper contributes to the state-of-the-art for on-demand mobility system charging management by developing an optimization framework that jointly considers vehicle relocation, fixed charging stations, and MCTs in an EV-based FFCS system. Our modeling framework provides an integrated optimization approach that jointly addresses idle EV charging, vehicle relocation, and MCT rebalancing to minimize both user inconvenience and operational time costs. The proposed framework is used to examine whether, and under which modeled conditions, the addition of MCTs reduces the weighted operational objective relative to a system relying only on fixed charging stations.

The rest of the paper is structured as follows. Section 2 reviews the literature, Section 3 presents the problem and the methodology, Section 4 reports the computational experiments, and Section 5 concludes the paper.

2. Literature review

Managing charging operations in EV-based FFCS systems introduces new operational challenges. Most studies on EV-based FFCS systems focus on fixed charging infrastructure (e.g., Cocca et al. (2019), Pantelidis et al. (2022) and Shui et al. (2024), among many others), integrating charging and vehicle relocation decisions to minimize system operating costs. However, fixed charging infrastructure suffers from several drawbacks, such as limited capacity, reduced operational flexibility, and uncertain waiting times, especially at public charging stations. In addition, vehicles must travel to predefined charging locations, which can increase vehicle downtime and reduce fleet availability during charging operations. In contrast, MCTs can travel to vehicles requiring charging and serve a wider range of locations, subject to MCT parking, travel-time, energy and charging capacity constraints (Afshar et al., 2020). This section reviews the concepts, technologies, and applications of mobile charging in EV-based on-demand mobility systems. For broader reviews of FFCS relocation models, see Illgen and Höck (2019) and Ma et al. (2019).

Concepts and technologies of mobile charging systems

Afshar et al. (2020) reviewed mobile charging technologies and classified different types of mobile charging systems based on their physical configuration and energy supply mechanisms. Among these, MCTs equipped with a mounted battery energy storage system are identified as a flexible charging solution, as they can travel to any EV's location in the service area and provide charging services. From a modeling perspective, the introduction of MCTs shifts part of the charging management problem from assigning EVs to fixed charging stations toward synchronized routing and scheduling decisions for the charging service of MCTs. Other mobile charging technologies include vehicle-to-vehicle (V2V) charging that transfers energy between EVs (Yan et al., 2024). MCTs can operate either as energy distribution units connected to fixed infrastructure or as stand-alone portable battery systems (Afshar et al., 2020). These solutions introduce additional flexibility compared to fixed charging stations by allocating charging capacity dynamically in space and time to meet EV charging demand.

Optimization models for mobile charging operations

MCT operations in EV-based on-demand mobility systems are commonly formulated as vehicle routing and service scheduling problems (Afshar et al., 2020). Afshar et al. (2022) developed a MILP model that assigns private EVs to either fixed or mobile charging stations with the objective of minimizing total charging costs and charging time. Their Chattanooga case study demonstrates that integrating mobile charging stations with fixed infrastructure can reduce total charging time and mitigate grid stress during peak demand hours. Qiao et al. (2025) proposed a bi-objective optimization model that jointly schedules and routes MCTs alongside fixed charging stations while minimizing MCT travel distance and maximizing service coverage. Their Shenzhen case study shows that MCTs improve system coverage and support infrastructure planning. However, both studies focus on private EVs and do not consider a carsharing context where vehicle relocation decisions need to be jointly considered.

Xiao et al. (2024) integrated MCTs into an EV-based vehicle routing problem with both EVs and MCT routes are jointly optimized to enable charging at coordinated locations. Their MILP model incorporates partial recharging, allowing EVs to be charged only with the required amount of energy and to wait for MCTs when necessary. This increases flexibility and reduces operational costs with high computational complexity due to interdependent routing and charging decisions between EVs and MCTs. Similarly, Zhang et al. (2025) considered MCTs in an electric station-based carsharing system to address the temporal and spatial imbalance of the charging demand. These MCTs travel between fixed charging stations to provide extra charging capacity and thus decrease waiting times at these stations. Their Hefei case study demonstrates that introducing MCTs can reduce charging waiting times and improve the operational performance of the carsharing system. However, this study considers deterministic customer demand, and the MILP model can be solved exactly with up to 40 customers, limiting its capability for real-world application.

Li et al. (2025) proposed an optimization-simulation framework that integrates MCTs into fixed charging stations to provide a flexible solution for private EV charging in urban areas. They integrate an EV charging demand forecasting model based on vehicle driving patterns. Then, an MCT dispatching policy is developed based on a reinforcement learning approach to dynamically adapt demand changes. Table A1 in **Appendix A** summarizes these studies and positions the contribution of the present research.

Research gaps and contributions

Most existing studies focus on MCT solutions for private EVs. The integration of MCTs and fixed charging stations within electric FFCS systems under stochastic customer demand remains underexplored. This study addresses this gap through the following contributions:

- We develop a mathematical model that integrates the flexibility of MCTs into the charging and relocation management of EV-based FFCS systems with the presence of fixed charging stations. The model aims to minimize the total system operational time costs, which capture both customer inconvenience and operator's operational costs. The proposed model simultaneously optimizes EV and MCT repositioning alongside charging schedules at fixed and mobile stations, drastically reducing EV recharging operational times and users' access times.
- We extend the node-charge graph approach (Pantelidis et al., 2022) that captures vehicle space-time-battery trajectories and accounts for the queueing delay approximation of customer demand as a facility allocation-relocation problem. The proposed extension corporates MCT positioning, energy and charging-capacity constraints, and the synchronization of EV and MCT arrivals with the presence of fixed charging stations.
- We apply the framework to a synthetic Manhattan-like 60-zone case study and compare the performance of the electric FFCS system with and without integrating MCTs under various operating conditions. A sensitivity analysis is conducted to assess the impact of (i) spatial distribution of idle vehicles; (ii) idle EV fleet size; (iii) spatial alignment between EV supply and customer demand; and (iv) objective function weights for different system cost components. The results illustrate the conditions under which MCT integration can reduce the weighted system objective.

3. Problem description and methodology

3.1. Problem description

We consider the rebalancing and charging problem of an EV-based FFCS system based on a queueing-based facility location modeling approach with mixed mobile charging vehicles and fixed charging stations. A central operator periodically controls the rebalancing and charging operations of a fleet of EVs in its service area. The entire planning horizon is divided into a sequence of equal-length time intervals (e.g., 1 hour) during which idle EVs are rebalanced and/or recharged to meet customer demand. The goal from an operator's perspective is to minimize a system cost function under various operational constraints, considering the trade-off between customer inconvenience and operator's costs. Customer demand is modeled through estimated arrival rates and queueing-based service-reliability constraints. The entire service area is divided into a set of zones where fixed charging stations are located in some zones and MCTs

can be repositioned between zones. For simplification, travel time between zones is measured as average travel times between zone centers. We assume that a fleet of homogeneous MCTs is available with limited battery size and a limited number of charging ports. EVs can be recharged at either public fixed charging stations or the fleet of MCTs. Using public fixed charging stations might require waiting, depending on the time of day. Expected waiting times at fixed charging stations are exogenous. Each MCT travels directly from its location at the beginning of the rebalancing epoch to the selected MCT charging zone. Each charger serves at most one EV during the epoch as an epoch-level service-capacity approximation.

The FFCS charging and rebalancing problem is to determine where to charge/reposition idle EVs, what type of charging facilities (public fixed charging stations or MCTs) to use, how much energy to charge for each EV, and where to reposition MCTs so as to minimize the total system cost function for each time interval. The system costs take into account the trade-offs of customers' inconvenience (access time to use the service) and operational costs of rebalancing for both EVs and MCTs. The joint staff scheduling for idle vehicle relocation is not considered. The formulation represents a single decision epoch and could form the basis of a future rolling-horizon implementation in which the model is repeatedly updated as vehicle, demand, and charging conditions change.

In the following, we first introduce the node-charge graph and then present the proposed MILP model considering both fixed charging stations and MCTs.

3.2. Node-charge graph approach

The FFCS charging and rebalancing optimization problem is formulated at the zonal level to coordinate the rebalancing and charging of EVs across zones, given zone-specific customer arrival and service rates with capacitated MCTs and fixed charging stations. To track a vehicle's SoC state over space and time, a node-charge graph modeling approach is adopted (Ma et al., 2019; Pantelidis et al., 2022). Figure B1 in **Appendix B** presents an illustrative example of the node-charge graph based modeling approach.

We apply the node-charge graph approach for modeling the charging and rebalancing problem with mixed (mobile and fixed) charging resources. Figure 1 presents a similar 5-zone example with fixed charging stations located at zones 1 and 5 and an MCT located at zone 4. Two idle EVs are located at zone 2 (vehicle 1 with SoC 20%+) and zone 3 (vehicle 2 with SoC 40%+), respectively. Depending on different system parameters and objective function settings, the best solution can be that vehicle 1 goes to charge at zone 1 to 60% (+ is dropped hereafter), and vehicle 2 goes to charge to 80% at zone 4, where an MCT is located at that zone, and then moves to zone 5. Different from the case presented in Figure 1, we further consider EV waiting times for charging by MCTs or at fixed charging stations and MCTs' rebalancing times/costs. MCTs' energy availability and number of chargers are taken into account as well in the charging operations.

Based on the node-charge graph approach, the charging and relocation decision problem can be formulated as a MILP model that jointly determines optimal vehicle relocation and charging (or discharging for MCTs) decisions for both types of vehicles. The following section presents the model formulation, including the sets, parameters, and decision variables, followed by the MILP formulation and a detailed description of the associated constraints.

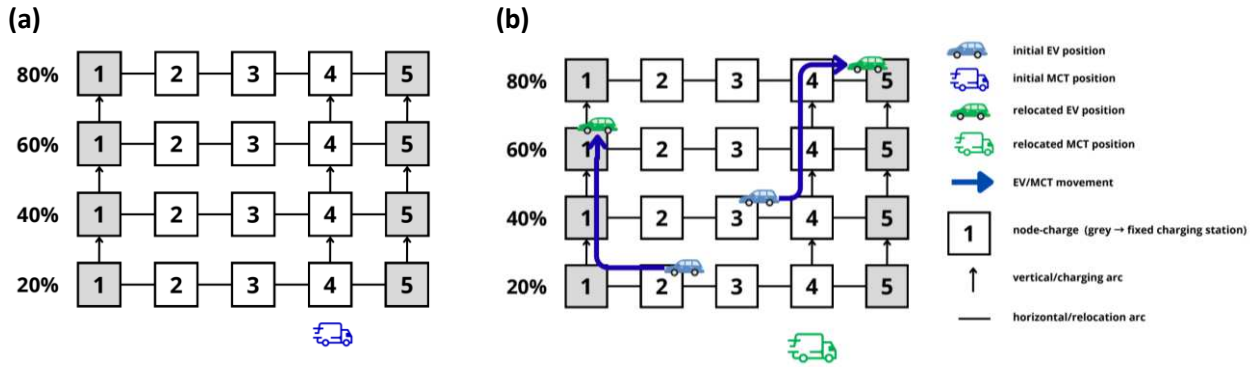


Figure 1. Node-charge graph representation with the presence of MCTs and fixed charging stations. (a) initial state (b) (idle) EV charging and rebalancing.

3.3. Model formulation

We use aggregate EV flow variables to represent how many idle EVs move between node-charges. However, MCT waiting times depend on the arrival time of individual EVs and trucks. Therefore, vehicle-specific variables are introduced only for the part of the model that requires synchronization between EVs and MCTs. The notation table is shown in **Appendix C**. The challenge lies in synchronizing MCT arrivals across zones to minimize EV waiting times when charging at these MCTs. The objective is to minimize total system time-costs as the weighted sum of users' access time, EV rebalancing time, truck relocation time, and EV charging waiting times for MCTs and at congested fixed charging stations. This needs to jointly consider the trade-off between rebalancing idle vehicles, MCTs, and users' access time to vehicles. The waiting time at fixed charging stations is assumed known at the start of a considered rebalancing interval based on historical data or by real-time information from the charging station operator. The objective function is formulated in terms of five decision variables. Variable X_{igjh} determines whether customer demand λ_{ig} at node-charge (i,g) is served by EVs located at the node-charge (j,h). Variable W_{igjh} represents the aggregate EV flow relocated from node-charges (i,g) to (j,h) that captures both EV relocation and charging operations. Variable Z_j^k indicates whether MCT k is positioned at zone j and thus accounts for MCT relocation from its initial location i_k^0 to j. Variable $R_{v,jghk}$ represents the waiting times of EV v for MCT k at zone j, depending on the arrival times of both types of vehicles at zone *j*. The variable p_{jgh} denotes the EV flow charging from one SoC level g to another level h at the fixed charging station at zone j incurring the (expected) waiting time at this fixed charging station.

The MILP model is formulated as follows.

$$\min\ \theta_0 \sum_{i\in N}\sum_{j\in N}\sum_{g\in H}\sum_{h\in H} \lambda_{ig}\,\tau_{ij} X_{igjh} + \theta_1 \sum_{((i,g),(j,h))\in A} t_{igjh}\, W_{igjh} + \theta_2 \sum_{k\in K}\sum_{i\in P}\sum_{j\in P} t^{MCT}_{i_k^0 j}\, Z_j^k \qquad (1)$$
$$+ \theta_3 \sum_{v\in V}\sum_{j\in P}\sum_{g\in H}\sum_{h\in H:\, h\geq g}\sum_{k\in K} R_{v,jghk} + \theta_4 \sum_{j\in F}\sum_{g\in H}\sum_{h\in H:\, h\geq g} p_{jgh}\,\omega_j$$

subject to Eqs. (2)-(41).

The objective function minimizes total system costs which is a weighted combination of five performance components. The first term represents the demand-weighted customer access time when customers at zone i demanding a charge level g are served by a vehicle at zone j with charge $h \geq g$. The second term represents the EV relovation and charging time, while the third captures MCT relocation times from their initial locations to assigned charging zones. The fourth term measures the time EVs wait for assigned MCTs to arrive. Finally, the last term is the expected waiting times of EVs when charging at fixed charging stations. The objective function is parameterized by $\theta_0, \theta_1, \theta_2, \theta_3, \theta_4$ to consider the trade-offs between competing system cost components.

Vehicle rebalancing, customer assignment, and queuing constraints: EV flow Constraints (2) and (3) require that customer demand for (i,g) is assigned to exactly one zone with the presence of idle vehicles with sufficient battery level $(h \geq g)$. Constraint (4) is an ordering constraint, which states that the m-th EV (server) can only be placed at a node-charge if the *(m−1)-th* EV is already present at the same location. Constraint (5) ensures that the total number of placed EVs equals the total number of initial idle EVs in the system. Constraint (6) is a piecewise linear queuing constraint adapted from Marianov and ReVelle (1996). The term $\sum_{i\in N}\sum_{g\in H}\lambda_{ig}\,X_{igjh}$ represents customers assigned to a vehicle at node-charge (j,h), while μ_{jh} is the service rate. $Y_{jh1}\rho_{\eta jh1} + \sum_{m=2}^{C} Y_{jhm}\left(\rho_{\eta jhm} - \rho_{\eta jh,m-1}\right)$ is a piecewise linear expression that enforces the utilization rate below a specified reliability threshold. This constraint ensures vehicle availability reliability. Given a user-defined reliability threshold, η, m idle EVs, and b customers in a queue, the parameter $\rho_{\eta jhm}$ can be obtained by solving the equation $\sum_{k=0}^{m-1}\left((m-k)m!\,m^b/k!\right)\left(1/\rho^{m+b+1-k}\right) \geq 1/(1-\eta)$ (Marianov and ReVelle, 1996). Constraint (7) ensures that demand can only be assigned to node-charges where at least one EV is placed. Constraint (8) and constraint (9) are binding constraints for inflow/outflow of EVs and the number of EVs after relocation. Constraint (10) guarantees that the inflow to a node-charge minus the

corresponding outflow and plus the initial number of idle EVs at that node-charge is equal to the number of EVs after relocation. M_1 is set as the fleet size B.

$$\sum_{j\in N}\sum_{h\in H:\, h\geq g} X_{igjh} = 1, \forall i \in N,\ g \in H \tag{2}$$

$$\sum_{j\in N}\sum_{h\in H:\, h< g} X_{igjh} = 0, \forall i \in N,\ g \in H \tag{3}$$

$$Y_{jhm} \leq Y_{jh,m-1}\,, \forall j \in N, \forall h \in H, m = 2, \dots, C \tag{4}$$

$$\sum_{j\in N}\sum_{h\in H}\sum_{m=1}^{C} Y_{jhm} = B \tag{5}$$

$$\sum_{i\in N}\sum_{g\in H} \lambda_{ig}\, X_{igjh} \leq \mu_{jh}\left[Y_{jh1}\rho_{\eta jh1} + \sum_{m=2}^{C} Y_{jhm}\left(\rho_{\eta jhm} - \rho_{\eta jh,m-1}\right)\right], \forall j \in N, h \in H \tag{6}$$

$$X_{igjh} \leq Y_{jh1}, \forall i, j \in N, \forall g, h \in H \tag{7}$$

$$\sum_{(j,h)\in A_{ig}^{-}} W_{jhig} - \sum_{(j,h)\in A_{ig}^{+}} W_{igjh} \leq M_1 Y_{ig1}, \forall (i,g) \in (N \times H)\backslash O \tag{8}$$

$$-\left(\sum_{(j,h)\in A_{ig}^{-}} W_{jhig} - \sum_{(j,h)\in A_{ig}^{+}} W_{igjh}\right) \leq M_1 Y_{ig1}, \forall (i,g) \in (N \times H)\backslash O \tag{9}$$

$$\sum_{(i,g)\in A_{jh}^{-}} W_{igjh} - \sum_{(i,g)\in A_{jh}^{+}} W_{jhig} + y_{jh} = \sum_{m=1}^{C} Y_{jhm}\,, \forall j \in N, h \in H \tag{10}$$

MCT rebalancing and EV charging: Constraint (11) states that each MCT is located at one of the relevant zones $P \subseteq N$. It ensures that each MCT is placed at exactly one (parking) zone at the end of a relocation decision time interval. Constraints (12)-(14) ensure that EVs can only be charged by an MCT if an MCT is assigned to that zone and if the truck has available charging capacity. Constraint (12) binds the total charging flow on the MCTs at a charging zone j from level g to level h Q_{jgh}^{k} with EV flow charging from g to h W_{jgjh}. Constraint (13) ensures that charging by truck k at zone j can only occur if that truck is physically present at that zone. Constraint (14) limits the number of EVs that can be charged simultaneously by a truck at a zone given its limited number of charging ports. Constraints (15) and (16) represent the charging flow at fixed charging stations. Constraint (15) ensures that the charging flow at a fixed charging station equals the EV flow between the charging states. Constraint (16) enforces the fixed charging station capacity constraint. Note that Constraints (2)-(10) and (15)-(16) are the same as the model of Pantelidis et al. (2022) that considers fixed charging stations for FFCS systems.

$$\sum_{j\in P} Z_j^k = 1, \forall k \in K \tag{11}$$

$$\sum_{k\,\in\, K} Q_{jgh}^{k} = W_{jgjh}, \forall j \in P, \forall g, h \in H\colon g < h \tag{12}$$

$$Q_{jgh}^{k} \leq M_1 Z_j^k, \forall k \in K, j \in P, \forall g, h \in H \tag{13}$$

$$\sum_{g\in H}\sum_{h\,\in\,H:\,h\,>\,g} W_{jgjh} \le \sum_{k\in K} lZ_j^k, \forall j \in P \tag{14}$$

$$\sum_{g'\le g}\sum_{h'\ge h} p_{jg'h'} = W_{jgjh}, \forall j \in F, \forall g,h \in H : h > g \tag{15}$$

$$\sum_{g}^{|H|-1}\sum_{h\,=\,g+1}^{H} p_{jgh} \le u_j, \forall j \in F, g,h \in H \tag{16}$$

Energy Delivery, Fleet Flow, and Timing Constraints: EV charging and energy constraints (17)-(19) enforce the energy delivery feasibility of the MCTs. Constraint (17) defines the total energy delivered by each truck q_k. Constraint (18) guarantees that the total energy delivered by an MCT does not exceed the maximum amount D_{max} that can be supplied within a decision epoch. Constraint (19) ensures that the energy delivered is constrained by the SoC of an MCT at the beginning of the decision epoch E_0^k. Constraint (20) binds the aggregate EV flow to EVs' routing decisions. Constraint (21) ensures that for each EV, it can be charged at fixed charging stations at most once. Constraints (22) and (23) enforce that each EV has one starting and one termination position at the node-charge graph. While constraint (24) defines the aggregate auxiliary variable y_{jh}. Constraint (25) ensures the flow conservation for each EV. For each EV and node-charge, the number of outgoing arcs minus that of incoming arcs should be equal to 1 at the initial node, -1 at the terminating node, and 0 elsewhere.

$$q_k = \sum_{j\in P}\sum_{g\in H}\sum_{h\,\in\,H:\,h\,>\,g} e_{gh}\, Q_{jgh}^k, \forall k \in K \tag{17}$$

$$q_k \le D_{max}, \forall k \in K \tag{18}$$

$$q_k \le E_0^k \forall k \in K \tag{19}$$

$$\sum_{v\in V} F_{igjh}^v = W_{igjh}, \forall i,j \in N, \forall g,h \in H \tag{20}$$

$$\sum_{j\in F}\sum_{g\in H}\sum_{h\,\in\,H:\,h\,>\,g} F_{jgjh}^v \le 1, \forall v \in V \tag{21}$$

$$\sum_{j\in N}\sum_{h\in H} n_{jh}^v = 1, \forall v \in V \tag{22}$$

$$\sum_{j\in N}\sum_{h\in H} \delta_{jh}^v = 1, \forall v \in V \tag{23}$$

$$\sum_{v\in V} \delta_{jh}^v = y_{jh}, \forall j \in N, h \in H \tag{24}$$

$$\sum_{(i,g)\in A_{jh}^+} F_{igjh}^v - \sum_{(i,g)\in A_{jh}^-} F_{igjh}^v = \delta_{jh}^v - n_{jh}^v, \forall v \in V, \forall\, j \in N, h \in H \tag{25}$$

Waiting Times and EV-MCT Assignment Constraints: Constraints (26)-(29) model the waiting times of EVs for MCTs. Constraint (26) ensures that if EV v is charged by an MCT k at zone j, exactly one MCT must be assigned to that EV at that zone. Constraint (27) ensures that an EV can only be charged by an MCT k at a zone if that MCT is present at that zone. Constraint (28) enforces that the charging flow of a truck at a zone equals the number of EVs charged by that truck at that zone. Constraint (29) determines the charging waiting time of an EV when the arrival time of the MCT is later than that of the EV. For synchronization between EVs and MCTs, an EV assigned to an MCT charging location is assumed to travel directly from its origin at the beginning of the rebalancing epoch to the selected MCT charging zone. The big-M approach is used to ensure

that constraint (29) is only activated if MCT k charges EV v at zone j from the charging state g to h. M_2 is set as the length of charging and rebalancing time interval (e.g., 1 hour).

$$\sum_{k\in K} S_{v,jghk} = F^{v}_{jgjh}, \forall v \in V, j \in P, \forall g,h \in H: h > g \quad (26)$$

$$S_{v,jghk} \leq Z^{k}_{j}, \forall v \in V, j \in P, \forall g,h \in H: h > g \quad (27)$$

$$\sum_{v\in V} S_{v,jghk} = Q^{k}_{jgh}, \forall j \in P, \forall g,h \in H: h > g, k \in K \quad (28)$$

$$Z^{k}_{j} t^{MCT}_{i^0_k j} - t^{v}_{j^0_v gjg} - M_2\left(1 - S_{v,jghk}\right) \leq R_{v,jghk}, \forall j \in P, k \in K, \forall g,h \in H: h > g, v \in V \quad (29)$$

Domain variables. Eqs. (30)-(41) are domain variables.

$$W_{igjh} \geq 0, \forall i,j \in N, \forall g,h \in H \quad (30)$$

$$X_{igjh} \in \{0,1\}, \forall i,j \in N, \forall g,h \in H \quad (31)$$

$$Y_{jhm} \in \{0,1\}, \forall j \in N, h \in H, m\ 1,2,\dots,C \quad (32)$$

$$Z^{k}_{j} \in \{0,1\}, \forall j \in P, k \in K \quad (33)$$

$$q_k \geq 0, \forall k \in K \quad (34)$$

$$Q^{k}_{jgh} \geq 0, \forall j \in P, k \in K, \forall g,h \in H \quad (35)$$

$$p_{jgh} \geq 0, \forall j \in F, \forall g,h \in H \quad (36)$$

$$F^{v}_{igjh} \in \{0,1\}, \forall v \in V, \left((j,h),(i,g)\right) \in A \quad (37)$$

$$n^{v}_{jh} \in \{0,1\}, \forall v \in V, j \in N, h \in H \quad (38)$$

$$\delta^{v}_{jh} \in \{0,1\}, \forall v \in V, j \in N, h \in H \quad (39)$$

$$R_{v,jghk} \geq 0, \forall j \in P, k \in K, \forall g,h \in H, v \in V \quad (40)$$

$$S_{v,jghk} \in \{0,1\}, \forall j \in P, k \in K, \forall g,h \in H, v \in V \quad (41)$$

4. Numerical experiments

In this section, we assess the system performance with and without MCTs under various scenarios on a Manhattan-like 60-zone area using synthetic data. We first illustrate the model output (see **Appendix D**) using a 10-zone example with four discretized SoC levels. The scalability of the model is evaluated in **Appendix E** on a set of larger test instances with up to 100 zones. The model is implemented in Julia using the Gurobi Optimizer (version 13.0) to solve the MILP models. The coding and model development were supported with ChatGPT. All experiments were conducted on a computer using an Intel Core i7-11800H processor (16 threads) and 64 GB of memory. The datasets, input parameters, and some outputs in this study are freely available at https://github.com/tym2021/data-optimization-of-mobile-charging-operations-for-e-carshare-.git.

We generate a synthetic case study based on a Manhattan-like area of 60 km² to test the proposed model and evaluate its benefit by comparing systems with and without MCTs. The study area is divided into 4x15 zones of 1 km² each (see Figure 2). The target SoC after recharge is discretized into four charging demand levels of 20%, 40%, 60%, and 80%, resulting in a 240-node-charge graph. The fleet size is 10 EVs. The initial EV positions are randomly distributed as indicated by the blue cars. There are three fixed charging stations, each with two charging ports, located at zones 18, 31, and 47 (zones with a grey border in Figure

2). Two MCTs are initially located at zone 29; each has two charging ports. The other model parameter settings are shown in Table E1 in Appendix E.

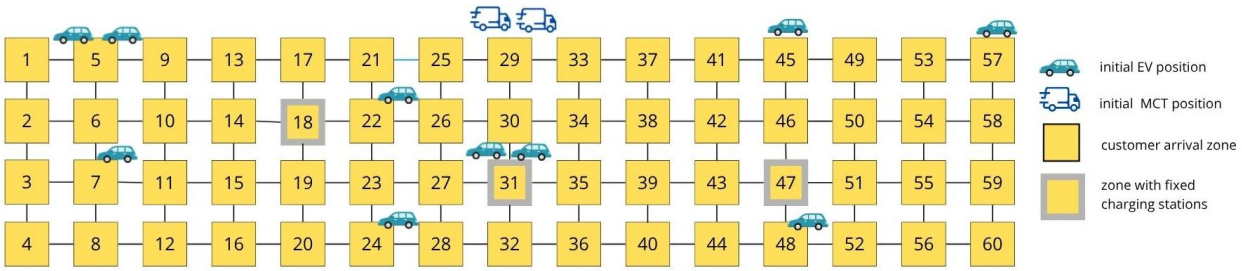


Figure 2. Test instance on a Manhattan-like 60-zone area with 10 EVs, 2 MCTs, and 3 fixed charging stations.

We define an indicator to quantify the gain of introducing MCTs to the system as follows.

$$MCT_{gain} = \frac{Z_{no_MCT} - Z_{MCT(1\ or\ 2)}}{Z_{no_MCT}}\ x\ 100 \tag{42}$$

where$Z$ is the objective function value of Eq. (1). This metric compares the objective values of different MCT scenarios with the baseline case without MCTs. The objective of the analysis is to determine whether the integration of MCTs improves system performance under different operating conditions. By comparing different cases under identical settings, the effect of integrating MCTs can be properly assessed.

To further assess the benefit of MCT integration under various conditions, we conduct the experiments with four scenarios. For each scenario, we consider three cases: a system without MCTs, a system with one MCT, and a system with two MCTs. All scenarios are solved within a 1% optimality gap.

a) **Base case**: serves as a benchmark to evaluate the benefits of integrating different numbers of MCTs. Figure 2 shows the initial state of the base case, including the initial EV positions, initial MCT positions, and the locations of the fixed charging stations.
b) **Impact of EV fleet size**: We change the size of the idle EV fleet from 10 to 40 EVs with two different initial locations (random or clustered) to evaluate the effect of EV fleet size.
c) **Impact of customer supply-demand alignment**: We set different spatial alignments between EV supply and customer demand from fully aligned to mismatched to evaluate the impact of different EV supply-demand conditions.
d) **Impact of objective function weights**: This scenario changes the objective function weights from the base case (equal weights on the different cost components) to a customer convenience-oriented strategy or an operator cost-oriented strategy.

4.1. Base case

We solve the model with three cases with 0, 1, and 2 MCTs and compare the key performance metrics of the system. Table 1 presents a comparison of the computational results for the three scenarios, including the MCT gains, objective function values, and the corresponding breakdown of these values. The results indicate that the integration of MCTs significantly enhances the system performance, with further improvements achieved through the deployment of additional MCTs. The objective value decreases from 1318.6 without MCTs to 1176.9 with one MCT and 1132.9 with two MCTs, corresponding to MCT gains of 10.74% and 14.09%, respectively. The reduction is primarily driven by customer access component, which decreases from 1123.6 minutes without MCTs to 911.9 minutes with one MCT and 837.9 minutes with two MCTs. At the same time, EV routing and charging time increases from 155.0 to 230.0 and 265.0 minutes. This increase can be explained by the additional routing and charging operations associated with the use of MCTs. Thus, in this instance, the model accepts additional EV and MCT movement to obtain a larger reduction in demand-weighted customer access time.

The number of charged EVs increases from four without MCTs to five in both MCT cases. Introducing MCTs also changes the allocation of charging operations: three EVs use fixed charging stations and two use the MCT in the one-MCT case, whereas one EV uses a fixed charging station and four use MCTs in the two-MCT case. The available MCT charging ports are therefore fully utilized in both configurations. These results show that mobile charging changes the joint charging and relocation solution and reduces reliance on fixed charging stations in the tested instance.

Figure 3 illustrates the final system state after optimization, showing the relocation and charging decisions for both EVs and MCTs in all three cases. Figure 3a shows the final state without MCTs, Figure 3b shows the final state in the case with one MCT, and Figure 3c illustrates the final state of the case with two MCTs. As can be observed, the final EV positions show only small differences across the three cases. This indicates that, **despite the integration of MCTs, EVs still tend to relocate towards the same preferred zones in all scenarios. These zones are likely more attractive due to higher customer demand, resulting in similar spatial distributions of EVs after optimization**

Table 1. Comparison of the MCT gains and different performance metrics for the scenarios with zero, one, and two MCTs (base case).

Measure	Without MCTs	With 1 MCT	With 2 MCTs
Objective function value	1318.6	1176.9	1132.9
Customer access time	1123.6	911.9	837.9
EV routing and charging time	155.0	230.0	265.0
MCT routing time	0.0	5.0	15.0
EV waiting time for MCTs	0.0	0.0	5.0
Charging waiting time at fixed charging stations	40.0	30.0	10.0
Total number of EVs charged	4	5	5
Number of EVs charged at fixed charging stations	4	3	1
Number of EVs charged by MCTs	0	2	4
Number of MCT relocations	0	1	2
CPU time	338	234	86
MCT gain	/	10.74%	14.09%

Remark: All scenarios are solved to optimality. Time is measured in minutes. CPU time is measured in seconds.

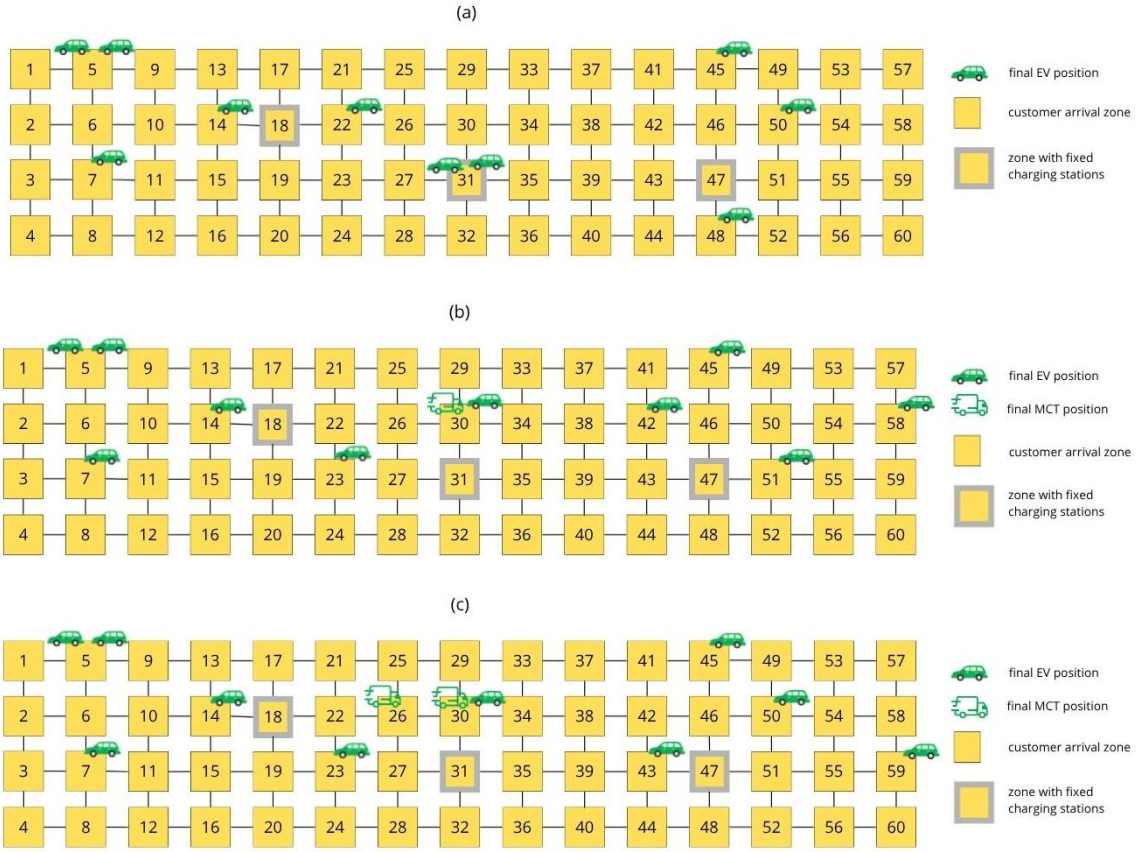


Figure 3. Final system state after optimization under different MCT configurations: (a) without MCTs, (b) with 1 MCT, and (c) with 2 MCTs.

4.2. Impact of idle EV fleet size

We consider three fleet size scenarios: 10, 20, and 40 idle EVs. Furthermore, two distinct spatial distributions of EVs are analyzed: a random distribution and a clustered distribution (see Figure 4 for the clustered distribution). For the clustered case, we consider a single central cluster. Table 2 shows that the relative benefit of MCT integration decreases as the idle EV fleet grows under both spatial distributions. With randomly distributed EVs, the gain from two MCTs decreases from 14.09% with 10 EVs to 1.34% with 40 EVs. For clustered EVs, the corresponding gain decreases from 9.59% to 0.13%. As the fleet grows, more sufficiently charged EVs are already available to serve expected demand, reducing the value of additional mobile-charging capacity.

The results also indicate diminishing marginal benefits from additional MCTs. In several scenarios, the second MCT provides only a limited improvement over the one-MCT configuration, particularly for larger fleet sizes. **This suggests that the operational value of additional MCT capacity becomes constrained once charging demand is sufficiently covered**. Overall, the results suggest that **MCTs are most valuable in systems with relatively small fleets, where charging decisions strongly affect vehicle availability and spatial coverage.**

Table 2. Comparison of the objective value and MCT gain for different fleet sizes with random and clustered EV locations.

Idle EV location	# of EVs	Objective			MCT gain	
		0 MCT	1 MCT	2 MCTs	1 MCT	2 MCTs
Random	10	1318.65	1176.95	1132.90	10.74%	14.09%
	20	1091.75	1012.35	999.90	7.27%	8.41%
	40	665.50	656.50	656.50	1.34%	1.34%
Clustered	10	1250.60	1164.40	1130.70	6.89%	9.59%

	20	974.85	944.70	935.90	3.09%	4.00%
	40	741.15	740.20	740.20	0.13%	0.13%

Remark: All scenarios are solved to optimality.

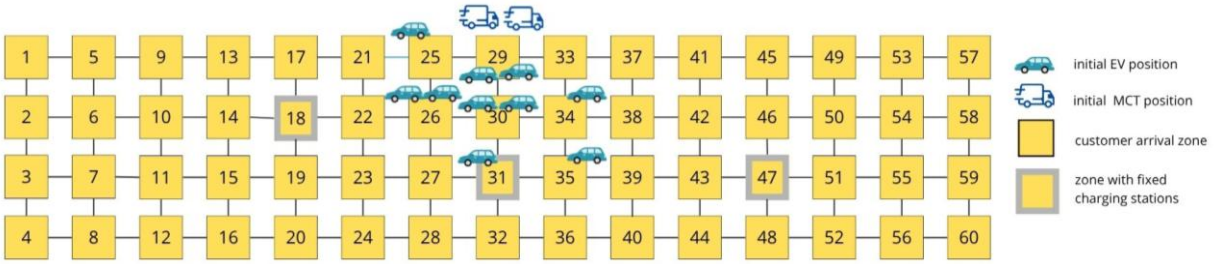


Figure 4. Initial idle EV positions for the clustered scenario.

4.3. Impact of spatial alignment between EV supply and customer demand

Spatial mismatch between EV supply (initial EV positions) and customer demand (arrival rates) can increase relocation needs. We therefore compare three demand patterns with EVs clustered around zones 8 and 54 (Figure 5): (i) aligned, with high-demand zones near EV clusters; (ii) partially misaligned, with demand distributed uniformly; and (iii) fully misaligned, with high demand concentrated around zone 30. Each pattern is evaluated with zero, one and two MCTs. Figure 5 shows these initial conditions, from alignment in panel (a) to full misalignment in panel (c). Note that across the three scenarios, the total customer arrival rate is kept constant to ensure a fair comparison.

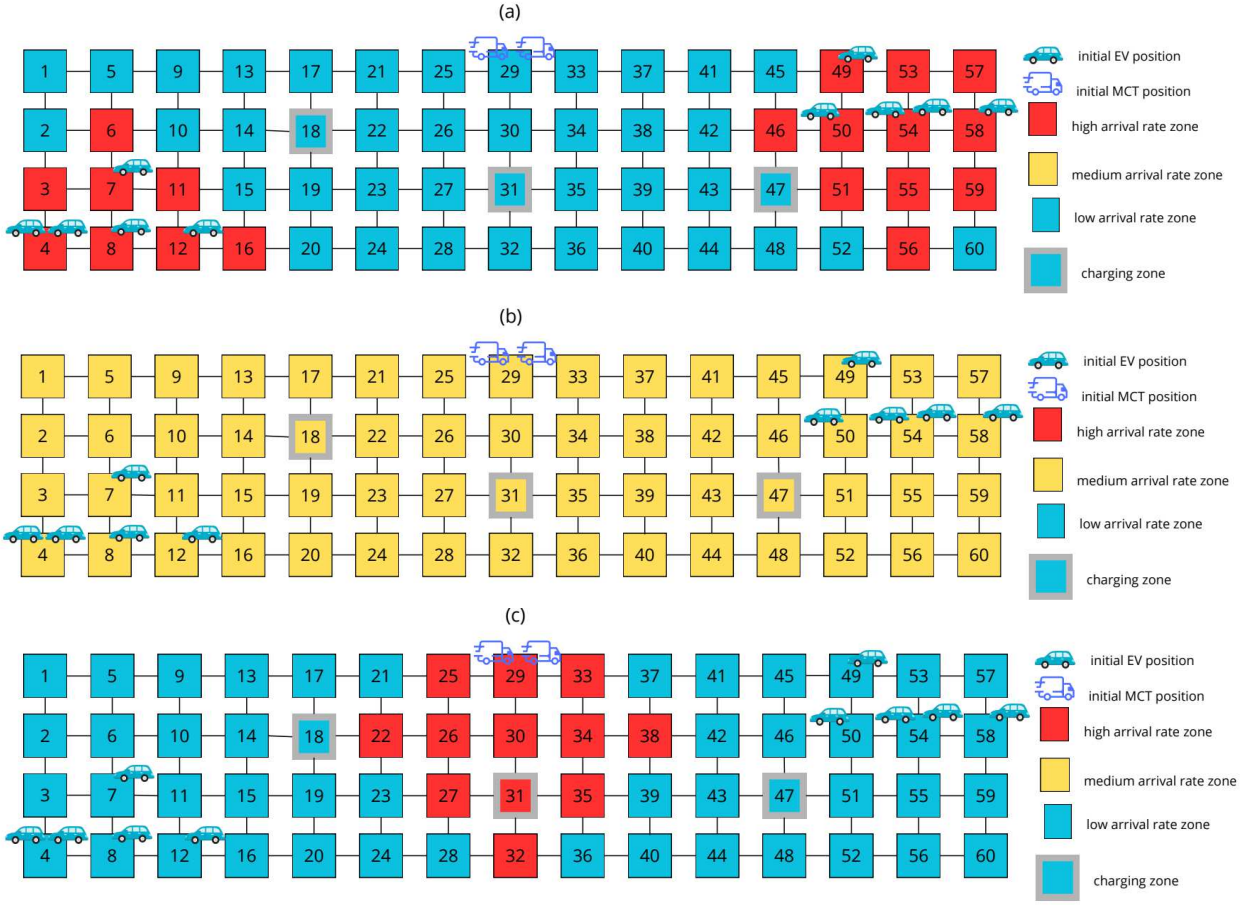


Figure 5. Initial EV locations in the three scenarios: (a) aligned, (b) partially misaligned, and (c) misaligned.

Table 3 compares the objective function values and MCT gains for the three scenarios, each with the integration of zero, one, and two MCTs. The results indicate that MCT gains increase with spatial mismatch between initial EV supply and customer demand. The gain from two MCTs rises from 2.90% in the aligned

scenario to 6.84% in the fully misaligned scenario. This suggests that mobile charging becomes more valuable when charging and relocation decisions are needed to overcome an unfavorable initial distribution. Nevertheless, the magnitude of the gain remains moderate, possibly because longer EV-MCT travel distances limit the flexibility provided by mobile charging.

Table 3. Comparison of the objective value and MCT gain under different spatial alignment scenarios.

Scenario	# of MCTs	Objective	MCT gain	CPU time
Aligned	0	1092.56	-	18
	1	1063.34	2.67%	64
	2	1060.91	2.90%	117
Partially	0	1139.15	-	47
	1	1091.20	4.21%	31
	2	1085.25	4.73%	85
Misaligned	0	1138.79	-	44
	1	1088.95	4.38%	45
	2	1060.91	6.84%	102

Remark: All scenarios are solved to optimality. CPU time is measured in seconds.

4.4. Impact of the objective function weights

In the previous analyses, all components of the objective function were assigned equal weights. However, in practice, system operators may prioritize different aspects of performance. This sensitivity analysis therefore evaluates how changes in the objective function weights influence the effectiveness of MCT integration. To assess its effect, four different weighting configurations are considered while keeping all other system parameters and configurations constant. A fleet of 10 EVs is used with a random distribution. The baseline case assigns equal weights to all components. This case is compared with three alternative configurations: an access-dominant case, where all weights (θ_1 to θ_4) are reduced equally from 1 to 0.5 to emphasize accessibility; a congestion-dominant case, where the weight associated with vehicle charging waiting time at fixed charging stations is increased; and an MCT-expensive case, where the weight on MCT routing time is increased from 1 to 5. Table 4 provides an overview of the objective weights in each configuration. For each configuration, the three different MCT settings are analyzed.

Table 4. Objective function weight configurations for different scenarios.

Scenario	θ_0	θ_1	θ_2	θ_3	θ_4
Baseline	1	1	1	1	1
Access-dominant	1	0.5	0.5	0.5	0.5
Congestion-dominant	1	1	1	1	5
MCT-expensive	1	1	5	1	1

Table 5 shows the objective value and the MCT gain for each case. The results indicate that the MCT gain depends on which aspect of performance is prioritized in the objective function. For the access-dominant case, the MCT gain is higher than the baseline case with 13.09% for one MCT and 18.72% for two MCTs. This is expected, as the customer access cost becomes relatively higher compared to the others, charging becomes more important. **The flexibility from MCTs helps the system performance**. The highest MCT gains are observed in the congestion-dominant case, with gains of 16.09% and 22.28% for one and two MCTs, respectively. In this scenario, waiting times at fixed charging stations are penalized more heavily, making MCT charging particularly attractive. This high MCT gain is expected, as the model prefers MCT charging over fixed charging. The lowest MCT gain is in the MCT-expensive case with only 9.61% for one MCT and 11.55% for two MCTs. Since the routing cost of MCTs is weighted more heavily, the model is less attracted to MCT charging. Consequently, the difference between systems without and with MCTs becomes smaller, reducing

the benefits of integrating MCTs. **Overall, the results demonstrate that the effectiveness of MCT integration is highly sensitive to the priorities set by the operator.**

Table 5. Comparison of the objective value and MCT gain for different scenarios.

Scenario	# of MCTs	Objective	MCT gain	CPU time
Baseline	0	1318.65	-	327
	1	1176.95	10.74%	271
	2	1132.90	14.09%	100
Access-dominant	0	1172.20	-	624
	1	1018.80	13.09%	684
	2	952.75	18.72%	642
Congestion-dominant	0	1462.00	-	112
	1	1226.80	16.09%	21
	2	1136.30	22.28%	84
MCT-expensive	0	1318.65	-	323
	1	1191.95	9.61%	232
	2	1166.30	11.55%	92

Remark: All scenarios are solved to optimality. CPU time is measured in seconds.

5. Conclusions and discussion

This study developed a mixed-integer linear programming model that jointly optimizes EV relocation, MCT movements, and allocation of charging operations between mobile and fixed facilities in an electric FFCS system . The model extends the node-charge graph modeling framework by incorporating MCT energy and charging capacity constraints and by synchronizing the arrival of EVs and MCTs within a decision epoch. The framework captures both the spatial distribution of vehicles and their battery states, while accounting for varying demand using the queuing delays through customer arrival rates, service rates, and the number of vehicles (servers) in the system.

In the synthetic 60-zone base case, introducing one and two MCTs reduced the weighted objective by 10.74% and 14.09%, respectively. These reductions were primarily associated with lower demand-weighted customer access time, although EV routing and charging time increased. The relative benefit of MCTs decreased as the idle fleet grew -- with 40 EVs, the estimated gains were between 0.13% and 1.34%, depending on the spatial distribution of vehicles. MCT gains were also higher when initial EV supply was more spatially misaligned with customer demand. Together, these results suggest that mobile charging is most potentially valuable when vehicle availability is constrained and when charging decisions strongly affect the spatial and battery-state distribution of the available fleet.

Although further research is required to incorporate more realistic operational assumptions, the proposed framework provides a first step toward integrated mobile charging management in FFCS systems and contributes to the broader literature on sustainable and flexible urban mobility systems. Several limitations should be acknowledged. For the EV fleet, homogeneous vehicles, and linear charging speeds simplify charging behavior. A minimum state of charge (SoC) of 15% is assumed in our study. This threshold is assumed to be sufficient for an EV to reach every zone within the operating area. Similarly, charging operations are modeled in a simplified way. MCTs are assumed to be fully charged at the start of the day with a large battery. In practice, MCTs equipped with smaller battery capacities may encounter operational constraints and require recharging throughout the operating period (Afshar et al., 2020). The computational analysis indicates that the exact formulation is suitable for small- and medium-sized instances, but solution performance becomes less consistent as the network and fleet sizes increase. Therefore, additional algorithmic development would be required before applying the model in large-scale or real-time operational settings.

Several operating parameters in the model can be derived from empirical operational data. These include the expected customer arrival rates and the waiting times at fixed charging stations. In practice, these parameters are dependent on the operating area and typically vary across decision epochs. For

example, waiting times at fixed charging stations may differ by station and time of day. Similarly, expected customer arrivals are influenced by various factors. Lastly, future research should incorporate real-world data to improve the parameter estimations, such as including investment costs, operational costs, labor costs, and infrastructure trade-offs in order to evaluate under which conditions MCTs become economically beneficial compared to additional fixed charging infrastructure.

References

1. Afshar, S., Macedo, P., Mohamed, F., & Disfani, V. (2020). A Literature Review on Mobile Charging Station Technology for Electric Vehicles. 2020 IEEE Transportation Electrification Conference & Expo (ITEC), 1184–1190. https://doi.org/10.1109/ITEC48692.2020.9161499
2. Afshar, S., Pecenak, Z. K., Barati, M., & Disfani, V. (2022). Mobile charging stations for EV charging management in urban areas: A case study in Chattanooga. Applied Energy, 325, 119901. https://doi.org/10.1016/j.apenergy.2022.119901
3. Cocca, M., Giordano, D., Mellia, M., & Vassio, L. (2019). Free floating electric car sharing design: Data driven optimisation. Pervasive and Mobile Computing, 55, 59–75. https://doi.org/10.1016/j.pmcj.2019.02.007
4. Fassio, E., Ciociola, A., Giordano, D., Noussan, M., Vassio, L., & Mellia, M. (2021). Environmental and Economic Comparison of ICEV and EV in Car Sharing. 2021 IEEE International Intelligent Transportation Systems Conference (ITSC), 1621–1626. https://doi.org/10.1109/ITSC48978.2021.9564578
5. Illgen, S., & Höck, M. (2019). Literature review of the vehicle relocation problem in one-way car sharing networks. *Transportation Research Part B: Methodological*, *120*, 193-204.
6. Li, P., Chen, S., Li, B., Wang, M., Li, C., & Hossain, M. S. (2025). Reinforcement Learning-Based Adaptive Mobile Charging Station Placements in Mobile-Fixed Charging Stations Collaboration Network. *IEEE Transactions on Intelligent Transportation Systems*, 27(3): 3773 - 3787
7. Ma, T. Y., Pantelidis, T., & Chow, J. Y. (2019). Optimal queueing-based rebalancing for one-way electric carsharing systems with stochastic demand. Paper presented in Transportation Research Board 98th Annual Meeting.
8. Marianov, V., & C. ReVelle (1996) The queueing maximal availability location problem: a model for the siting of emergency vehicles. European Journal of Operational Research, 1996. 93(1): 110-120.
9. Nijland, H., & Van Meerkerk, J. (2017). Mobility and environmental impacts of car sharing in the Netherlands. Environmental Innovation and Societal Transitions, 23, 84–91. https://doi.org/10.1016/j.eist.2017.02.001
10. Pantelidis, T. P., Li, L., Ma, T.-Y., Chow, J. Y. J., & Jabari, S. E. G. (2022). A Node-Charge Graph-Based Online Carshare Rebalancing Policy with Capacitated Electric Charging. Transportation Science, 56(3), 654–676. https://doi.org/10.1287/trsc.2021.1058
11. Qiao, D., Wang, G., & Xu, M. (2025) Mobile charging service optimization for electric vehicles, Transportation Letters, 17:8, 1375-1389, DOI: 10.1080/19427867.2024.2448783
12. Roni, M. S., Yi, Z., & Smart, J. G. (2019). Optimal charging management and infrastructure planning for free-floating shared electric vehicles. Transportation Research Part D: Transport and Environment, 76, 155–175. https://doi.org/10.1016/j.trd.2019.09.021
13. Shui, C. S., Chu, J. C., Lin, S.-C., & Shih, C.-H. (2024). Optimization of vehicle charging and dynamic relocation in free-floating electric carsharing systems with advanced reservations. Computers & Industrial Engineering, 190, 110072. https://doi.org/10.1016/j.cie.2024.110072
14. Xiao, J., Liu, X., Liu, T., Li, N., & Martinez-Sykora, A. (2024). The electric vehicle routing problem with synchronized mobile partial recharging and non-strict waiting strategy. Annals of Operations Research. https://doi.org/10.1007/s10479-024-06069-3
15. Yan, Y., Lin, X., He, F., & Wang, D. Z. W. (2024). Dynamic Operations of a Mobile Charging Crowdsourcing Platform. Transportation Science, 58(5), 995–1015. https://doi.org/10.1287/trsc.2023.0126

16. Zhang, L., Chen, T., Yao, B., Yu, B., & Wang, Y. (2025). Routing and charging scheduling for the electric carsharing system with mobile charging vehicles. Omega, 131, 103211. https://doi.org/10.1016/j.omega.2024.103211

Supplementary Files

This is a list of supplementary files associated with this preprint. Click to download.

- AppendixETRRf.docx